Feedback control and quantum error correction assisted quantum multi-parameter estimation

Hai-Yuan Hong(洪海源)[1,†], Xiu-Juan Lu(鲁秀娟)[2,†], and Sen Kuang(匡森)[1,‡]

[1] *Department of Automation, University of Science and Technology of China, Hefei* 230027, *China*
[2] *Department of Mechanical Engineering, The University of Hong Kong, Hong Kong* 999077, *China*

(Received 13 April 2022; revised manuscript received 29 July 2022; accepted manuscript online 5 August 2022)

Quantum metrology provides a fundamental limit on the precision of multi-parameter estimation, called the Heisenberg limit, which has been achieved in noiseless quantum systems. However, for systems subject to noises, it is hard to achieve this limit since noises are inclined to destroy quantum coherence and entanglement. In this paper, a combined control scheme with feedback and quantum error correction (QEC) is proposed to achieve the Heisenberg limit in the presence of spontaneous emission, where the feedback control is used to protect a stabilizer code space containing an optimal probe state and an additional control is applied to eliminate the measurement incompatibility among three parameters. Although an ancilla system is necessary for the preparation of the optimal probe state, our scheme does not require the ancilla system to be noiseless. In addition, the control scheme in this paper has a low-dimensional code space. For the three components of a magnetic field, it can achieve the highest estimation precision with only a 2-dimensional code space, while at least a 4-dimensional code space is required in the common optimal error correction protocols.

Keywords: quantum multi-parameter estimation, feedback control, quantum error correction, Heisenberg limit

PACS: 06.20.–f, 03.65.Yz, 03.67.Pp, 03.67.–a **DOI:** 10.1088/1674-1056/ac8721

1. Introduction

Quantum metrology exploits some unique properties of quantum systems, such as entanglement, superposition and coherence, to provide higher measurement precision than classical metrological schemes.[1–3] Due to high resolution and high sensitivity, they have been widely used in the field of high-precision measurement and sensing, ranging from magnetometry, frequency spectroscopy, gravitational wave detection, Hamiltonian identification to quantum imaging, quantum biology, and so on.[4–10]

Quantum parameter estimation aims to obtain the true values of estimated parameters that are encoded in the state of a quantum system through the interaction of the quantum system with an external signal of interest. A complete quantum parameter estimation process includes three steps: the preparation of an initial probe state, the encoding process of parameters to be estimated, and the measurement of the final state. Most existing studies focus on the determination of an optimal initial probe state and optimal measurements.[11–14] In recent years, it has been realized that control can be used to change the dynamics of the system and further improve the estimation precision of parameters.[15–22]

Control is an important and effective resource in quantum parameter estimation. For example, optimal control has been used to improve the estimation accuracy of the magnetic field and to image nanoscale magnetic fields.[23,24] For unitary dynamics, quantum coherent control was used to achieve the highest estimation accuracy of a parameter by encoding it into a time-independent Hamiltonian.[18] For a parameter contained in the time-dependent Hamiltonian of a quantum sensor, Pang *et al.*[19] showed that the highest measurement accuracy of the parameter can be achieved by adaptive control. In view of the fact that a practical quantum system is often affected by noises, which greatly reduce the precision limit of estimation, Liu *et al.*[20] used the gradient-based optimal control method to suppress the negative effect of noises on the estimation accuracy. However, as the system dimension increases, the gradient-based optimization methodology becomes more and more difficult since the gradient update requires a new simulation of the system dynamics. To solve this problem, reinforcement learning (RL) was proposed, e.g., in Ref. [21]. By the generalization ability of RL, the optimal control obtained at a certain value of the parameter is also applicable to the other values around it, which avoids the re-training process after the parameter is updated. For high-dimensional systems, the situation becomes more complex. Thus, a relatively simple and effective scheme with feedback control and QEC can be considered to improve the estimation accuracy of the parameter to be estimated in the noisy system.

Feedback control, which usually uses the measurement information to manipulate a system, is an effective method to suppress the decoherence of the system and has been used in the generation of robust entanglement in open quantum systems,[25] the protection of quantum correlation,[26] etc. In

[†] These authors contributed equally to this work.
[‡] Corresponding author. E-mail: skuang@ustc.edu.cn
© 2023 Chinese Physical Society and IOP Publishing Ltd

the field of parameter estimation, feedback control has also been widely investigated to improve the estimation accuracy of the decoherence parameter[27] and physical quantities such as phase and magnetic field strength.[28–30] It should be noted that only the case of estimating a single parameter has been considered at present. However, single-parameter models are usually an oversimplification of real-life metrological setups. As a matter of fact, there are many scenarios involving the simultaneous estimation of multiple parameters, e.g., simultaneous estimation of multiple phases,[31,32] and simultaneous estimation of phase and noise.[33,34] Recent studies have shown that the simultaneous estimation of multiple parameters may achieve a higher accuracy than the individual estimation of each parameter, which prompts the development of quantum multi-parameter estimation.[35,36]

In quantum multi-parameter estimation scenarios, control is still an important resource. For example, a sequence feedback control scheme was proposed in Ref. [37], which solves the problem that the incompatibility of optimal measurements on various parameters hinders their simultaneous high-precision estimation and achieves a joint quantum-enhanced measurement of all three components of a magnetic field. Hou *et al.*[38] further achieved this scheme by experiment. On the other hand, in order to restore the Heisenberg limit (HL), quantum error correction (QEC) has been proposed for general non-unitary dynamics.[39] As a special control means, QEC is an important approach to reduce noises in quantum channels. In recent years, it has shown a powerful ability to the quantum parameter estimation in noisy environments.[40–44] However, the HL can only be reached, e.g., in some special cases of dephasing and erasure noises.

In this paper, we propose a new combined control scheme with feedback and QEC to improve the accuracy of quantum multi-parameter estimation, where the estimation precision can reach the HL in the presence of spontaneous emission. Compared with the pure QEC schemes, our combined control scheme does not require the ancilla system that is used to construct an optimal probe state to be noiseless, which reduces the experimental requirements. Generally, feedback and QEC are two important tools to combat with the environment-induced decoherence. The former applies feedback control based on continuous measurement to suppress noises and the latter corrects errors by performing projective measurement. In our scheme, we combine these two tools. An immediate benefit of this combination is that the dimensionality of the correction code space can be reduced. For the Hamiltonian parameter estimation in two-qubit systems, an optimal error correction protocol requires the dimensionality of the code space to be at least $P+1$ when the number of parameters is P,[39] while our scheme can greatly reduces this dimensionality. For example, for the simultaneous estimation of the three parameters of a magnetic field, the code space is 4-dimensional in the optimal error correction protocol while the 2-dimensional code space is sufficient to achieve the highest estimation precision of the three components of the magnetic field simultaneously in our scheme. Accordingly, our scheme is at the expense of reducing the kinds of errors that can be corrected (one type of stabilizer code usually corrects one type of errors), and the information of errors needs to be accurately detected.

This paper is organized as follows. Some preliminaries for quantum multi-parameter estimation and the methods used in this work, including feedback control and quantum error correction, are introduced in Section 2. In Section 3, we present our control scheme in detail. Finally, we summarize our results in Section 4. Some necessary details are provided in Appendices A and B.

2. Backgrounds and preliminaries

2.1. Quantum multi-parameter estimation

When the detected signal contains p parameters, denoted as the vector $\boldsymbol{x} = [x_1, \ldots, x_p]^{\mathrm{T}} \in R^p$, these parameters can be encoded into a quantum state $\rho(\boldsymbol{x})$ through the interaction of the quantum system with the external signal. A set of measurement results is obtained by applying a set of measurement operators M_m ($M_m \geq 0$, $\sum_m M_m = I$) to the multiple copies of the quantum state $\rho(\boldsymbol{x})$. Then, we can construct an estimator function $\hat{\boldsymbol{x}}$ (a $p \times 1$ vector) for the true value $\boldsymbol{x}$ based on the measurement results. The performance of the estimator function $\hat{\boldsymbol{x}}$ can can be written as[45]

$$\sum(\hat{\boldsymbol{x}}) = \sum_m P_{m|\boldsymbol{x}} [\boldsymbol{x} - \hat{\boldsymbol{x}}] \cdot [\boldsymbol{x} - \hat{\boldsymbol{x}}]^{\mathrm{T}}, \tag{1}$$

where $P_{m|\boldsymbol{x}} = \mathrm{Tr}(\rho(\boldsymbol{x}) M_m)$ represents the conditional probability and m is the measurement result. In this paper, we use the notation $\mathrm{tr}(\cdot)$ to stand for the matrix trace associated with the parameter space and the notation $\mathrm{Tr}(\cdot)$ to denote the trace with respect to the relevant Hilbert space of quantum states. Each diagonal element of $\sum(\hat{\boldsymbol{x}})$ represents the variance of the estimator of the corresponding parameter while the off-diagonal element represents the covariance between different parameters.

According to the Cramér–Rao bound, the covariance matrix $\sum(\hat{\boldsymbol{x}})$ is bounded as[45]

$$\sum(\hat{\boldsymbol{x}}) \geq F_{\mathrm{cl}}^{-1}, \tag{2}$$

where F_{cl} denotes the classical Fischer information matrix (CFIM). It represents the achievable precision in multi-parameter estimation, defined as $F_{\mathrm{cl}} = \sum_m \frac{[\nabla P_{m|\boldsymbol{x}}] \cdot [\nabla P_{m|\boldsymbol{x}}]^{\mathrm{T}}}{P_{m|\boldsymbol{x}}}$, where ∇ denotes the gradient operator with respect to $\boldsymbol{x}$. The (i,j)th entry of the CFIM is give by

$$(F_{\mathrm{cl}})_{ij} = \sum_m \frac{(\partial_{\theta_i} P_{m|\boldsymbol{x}})(\partial_{\theta_j} P_{m|\boldsymbol{x}})}{P_{m|\boldsymbol{x}}}. \tag{3}$$

In order to measure the precision of multi-parameter estimation intuitively, we introduce a scalar cost function, defined as[46]

$$C = \mathrm{tr}\left(W \sum(\hat{\boldsymbol{x}})\right), \tag{4}$$

where W is a $p \times p$ real symmetric positive definite weight matrix, and therefore C is also called weighted mean square error (WMSE). Now, we can trace F_{cl}^{-1} with the weight matrix W to obtain the corresponding scalar bound $C_{\mathrm{F}} = \mathrm{tr}(WF_{\mathrm{cl}}^{-1})$, i.e., the classical Cramér–Rao bound (CCRB). It is easily attainable. From Eq. (2), the WMSE is lower bounded through the generalization of the matrix Cramér-Rao bound, i.e.,

$$C \geq C_{\mathrm{F}}. \tag{5}$$

For simplicity, in this paper we take $W = I$, where I is the identity matrix. Then, we can obtain

$$C = \sum_{j=1}^{p} \delta x_j^2, \tag{6}$$

where δx_j^2 represents the variance of the estimator for the jth parameter. Here, the achievability of the HL means that there exists a set of protocols, including the optimal probe state, the control scheme, and the optimal measurement, such that $C \propto 1/T^2$, where T is the total sensing time. This equals that the estimation precision of each parameter reaches the HL.

2.2. Quantum feedback control

Quantum feedback control manipulates the system by employing the information obtained from the continuous measurement. The dynamics of the measured system can be described by a Markov master equation, which is the average dynamics over all possible measurement records and is therefore not random. The form of the master equation is not unique due to the different ways of collecting system information from the environment. For example, there are master equations based on direct photodetection, and master equations based on homodyne detection. In this paper, we mainly consider the master equation based on direct photodetection, and the detection process can be described by two Kraus operators.[47] It is assumed that the change of the state of the system in time interval $\mathrm{d}t$ under the environment-induced error can be described by a jump operator c. This means that we can use a Kraus operator $\Omega_1 = c\sqrt{\mathrm{d}t}$ to represent the process of jump. The other Kraus operator is $\Omega_0 = I - \Omega_1^{\dagger}\Omega_1/2 - \mathrm{i}H_0\mathrm{d}t$. By this way, the master equation without feedback can be written as[47]

$$\rho(t+\mathrm{d}t) = \Omega_0\rho(t)\Omega_0^{\dagger} + \Omega_1\rho(t)\Omega_1^{\dagger}. \tag{7}$$

The first term on the right-hand side of Eq. (7) represents the evolution of the system when no photons are detected, and the second term corresponds to the system evolution when photons are detected. In the feedback scheme based on photodetection measurement, feedback control is applied as soon as an emitted photon is detected by the detector. We use a special unitary operator U to represent the feedback control. Then, the master equation of the system with the feedback control can be obtained as

$$\begin{aligned} \mathrm{d}\rho(t) &= \Omega_0\rho(t)\Omega_0^{\dagger} - \rho(t) + U\Omega_1\rho(t)\Omega_1^{\dagger}U^{\dagger} \\ &= -\mathrm{i}[H_0, \rho(t)]\mathrm{d}t + \mathcal{D}[U\,c]\rho(t)\mathrm{d}t, \end{aligned} \tag{8}$$

where the superoperator $\mathcal{D}[A]\rho = A\rho A^{\dagger} - \frac{1}{2}(A^{\dagger}A\rho + \rho A^{\dagger}A)$ represents the decoherence caused by the environment.

2.3. Quantum error correction

Quantum error-correcting codes are specifically designed to protect unknown quantum states, in which stabilizer codes are a very important class. The introduction of the notion of stabilizer not only helps discover more quantum error correction codes, but also makes the theory of quantum error-correction codes more systematic.[48] In this paper, we use this type of error-correcting codes.

Suppose that the stabilizer code is encoded into k qubits of n qubits and S represents the stabilizer of the code. To describe the stabilizer code, we firstly define a Pauli group $G_n = \{\pm 1, \pm \mathrm{i}\} \otimes \{I, X, Y, Z\}^{\otimes n}$, where X, Y, and Z denote the Pauli matrices σ_x, σ_y, and σ_z, respectively, and the notation $\otimes$ denotes the Kronecker product. S is a 2^{n-k}-dimensional Abelian subgroup of the Pauli group G_n, which means that any element in S satisfies the commutation relation. It is enough to describe S with $n-k$ generators. The code space $C(S)$ is an eigenspace of eigenvectors corresponding to the eigenvalue $+1$ of all operators in S, and its dimension is 2^k. Hence, one can think that the system is encoded into k qubits, instead of n qubits.

The general protocol for the stabilizer code begins with the measurement of stabilizer generators. The projection measurement discretizes the error that has occurred in one of 2^{n-k} error syndromes. After obtaining the information of what error syndrome occurred, the corresponding unitary recovery operator is applied immediately to correct the error, thereby protecting the system state in the code space. In this protocol, the system needs to be entangled with a meter in order to diagnose the error syndrome by directly measuring the meter. In this paper, we employ continuous measurements and feedback control to correct the error instead of the projective measurements and fast unitary gates. By this means, the error syndrome can be diagnosed by directly measuring the environment without entangling with the meter.

3. Feedback control and QEC for multi-parameter estimation

In this section, we focus on the simultaneous estimation of multiple parameters. We use a feedback control scheme combined with error correction to improve their simultaneous estimation precision in the presence of spontaneous emission. We consider the simultaneous estimation of the three components of a magnetic field in a two-qubit system. This is a very classic problem in the Hamiltonian parameter estimation and quantum sensing.

Consider a two-qubit system, where one qubit is used to sense the parameters to be estimated and the other qubit acts as an ancilla system, which is not required to be noiseless. We use the notation X_j, Y_j, and Z_j to denote the Pauli operators σ_x, σ_y, and σ_z acting on the jth qubit. The Hamiltonian of the system sensing a magnetic field can be expressed as

$$H_0 = x_1 X_1 + x_2 Y_1 + x_3 Z_1 \triangleq \boldsymbol{B}\cdot\boldsymbol{\sigma}^{(1)}, \tag{9}$$

where x_1, x_2, and x_3 represent the magnitudes of the three components of the magnetic field in the directions of x, y, and z and are the parameters to be estimated; $\boldsymbol{\sigma}^{(1)} = (X_1, Y_1, Z_1)$; $\boldsymbol{B} = (x_1, x_2, x_3) \triangleq (B\sin\theta\cos\phi, B\sin\theta\sin\phi, B\cos\theta)$ with B and (θ,ϕ) being the magnitude and direction angles of the magnetic field in the polar coordinate system.

The optimal probe state for this system is any maximally entangled state (see Appendix A for detailed derivation). In this paper, we choose $|\psi_0\rangle = \frac{1}{\sqrt{2}}(|00\rangle - |11\rangle)$ as the probe state. Accordingly, the codewords of the stabilizer code can be selected as

$$\begin{cases} |0_{\rm c}\rangle &= (|00\rangle - |11\rangle)/\sqrt{2}, \\ |1_{\rm c}\rangle &= (|01\rangle + |10\rangle)/\sqrt{2}. \end{cases} \tag{10}$$

By this means, the optimal initial probe state is located in the code space, which is one of the conditions of our scheme. In the stabilizer representation, the generator of the stabilizer corresponding to the code is $Y\otimes Y$, that is, the codewords in Eq. (10) are all the eigenstates corresponding to the eigenvalue $+1$ of $Y\otimes Y$.

Since the probe system is affected by the spontaneous emission noise, according to Subsection 2.2, the jump operator corresponding to the noises on the jth qubit is

$$\Omega_j = \sqrt{\gamma_j {\rm d}t}(X_j - {\rm i}Y_j), \tag{11}$$

where γ_j represents the damping rate of the jth qubit. The master equation (7) without any controls can be rewritten as

$$\dot{\rho} = -{\rm i}[H_0, \rho] + \sum_{j=1}^{2} \gamma_j \mathcal{D}[X_j - {\rm i}Y_j]\rho. \tag{12}$$

Assume that the probe system has a spontaneous emission error on the first qubit. Then, the codewords of the stabilizer code immediately become

$$\begin{cases} \Omega_1|0_{\rm c}\rangle = -\sqrt{2\gamma_1 {\rm d}t}|01\rangle, \\ \Omega_1|1_{\rm c}\rangle = \sqrt{2\gamma_1 {\rm d}t}|00\rangle. \end{cases} \tag{13}$$

The encoded state in the code space can be represented as $\rho = (a|0_{\rm c}\rangle + b|1_{\rm c}\rangle)(a|0_{\rm c}\rangle + b|1_{\rm c}\rangle)^\dagger$, where a and b are complex numbers. Then, we have $\Omega_1\,\rho\,\Omega_1^\dagger = 2\,\gamma_1\,{\rm d}t\,(a\,a^*\,|01\rangle\langle 01| - a\,b^*\,|01\rangle\langle 00| - a^*\,b|00\rangle\langle 01| + b\,b^*|00\rangle\langle 00|)$. A similar change occurs when spontaneous emission occurs on the second qubit. It is not hard to see that the spontaneous emission noise will cause the state originally in the stabilizer code space to jump out of the code space, so that the coherence and entanglement that are helpful in enhancing the precision of parameter estimation will gradually disappear. To suppress this negative effect of the noise, we use a continuous measurement to obtain the information about the time and location of a spontaneous emission, and then immediately apply a set of unitary recovery operators to protect the code space from the noise. It is known that there exists a set of unitary recovery operators that can correct the error as long as the stabilizer code and the error satisfy the following sufficient and necessary condition[49]

$$\langle\phi_k|\Omega_j^\dagger\Omega_j|\phi_l\rangle = c_j\delta_{kl}, \tag{14}$$

where $|\phi_k\rangle$ and $|\phi_l\rangle$ are the elements of an orthonormal basis of the stabilizer code, and c_j is a constant. Obviously, the codewords $|0_{\rm c}\rangle$ and $|1_{\rm c}\rangle$ in Eq. (10) satisfy the conditions in Eq. (14). Therefore, there exists a set of unitary recovery operators that can correct this spontaneous emission error.

For the stabilizer code selected in this paper, if the unitary recovery operators can return the codewords in Eq. (13) to the code space, that is, $U_1\Omega_1|0_c\rangle \to |0_{\rm c}\rangle, U_1\Omega_1|1_{\rm c}\rangle \to |1_{\rm c}\rangle$, then it is not difficult to obtain $U_1\Omega_1\rho\Omega_1^\dagger U_1^\dagger \to 2\gamma_1{\rm d}t\rho$. That is to say, the role of $U_1\Omega_1\rho\Omega_1^\dagger U_1^\dagger$ in the code space can be regarded as an identity matrix. By this way, the jump error induced by spontaneous emission can be corrected. Hence, the unitary recovery operators can be chosen as

$$\begin{cases} U_1 = \frac{1}{\sqrt{2}}(X\otimes I + {\rm i}I\otimes Y), \\ U_2 = \frac{1}{\sqrt{2}}(I\otimes X + {\rm i}Y\otimes I). \end{cases} \tag{15}$$

Here, U_1 and U_2 correspond to the feedback control in Eq. (8). The set of unitary recovery operators can be realized by the following feedback Hamiltonian

$$H_{\rm fb} = \sum_{j=1}^{2} \frac{{\rm d}N_j(t)}{{\rm d}t} V_j, \tag{16}$$

where N_j is the number of photons emitted by the qubit j, and $U_j = {\rm e}^{-{\rm i}V_j}$.

However, the existence of the unitary recovery operators is only a necessary condition for returning the encoded state to the code space. The non-trivial evolution between spontaneous emissions can cause the encoded state to jump out of the code space, and therefore destroys the entanglement and

coherence and reduces the precision of parameter estimation. According to Subsection 2.2, such an evolution can be described by the following Kraus operator:

$$\begin{aligned}\Omega_0 &= I\otimes I-\sum_{j=1}^{2}\Omega_j^{\dagger}\Omega_j/2-\mathrm{i}H_0\mathrm{d}t\\ &= I\otimes I(1-(\gamma_1+\gamma_2)\mathrm{d}t)-\gamma_1 Z\otimes I\mathrm{d}t\\ &\quad-\gamma_2 I\otimes Z\mathrm{d}t-\mathrm{i}H_0\mathrm{d}t.\end{aligned}\tag{17}$$

In order to solve the problems caused by the non-trivial evolution, we introduce a driving Hamiltonian as

$$H_{\mathrm{d}}=\gamma_1 X\otimes Y+\gamma_2 Y\otimes X.\tag{18}$$

Thus, Eq. (17) can be rewritten as

$$\begin{aligned}\Omega_0 &= I\otimes I-\sum_{j=1}^{2}\Omega_j^{\dagger}\Omega_j/2-\mathrm{i}(H_0+H_{\mathrm{d}})\mathrm{d}t\\ &= I\otimes I(1-(\gamma_1+\gamma_2)\mathrm{d}t)-\gamma_1\mathrm{d}tZ\otimes I(I\otimes I-Y\otimes Y)\\ &\quad-\gamma_2\mathrm{d}tI\otimes Z(I\otimes I-Y\otimes Y)-\mathrm{i}H_0\mathrm{d}t.\end{aligned}\tag{19}$$

Since $(I\otimes I-Y\otimes Y)\mid 0_{\mathrm{c}}\rangle=(I\otimes I-Y\otimes Y)\mid 1_{\mathrm{c}}\rangle=\mathbf{0}$, for any quantum state ρ in code space, we have $(I\otimes I-Y\otimes Y)\rho=\mathbf{0}$. Therefore, the nonunitary part in the non-trivial evolution can be eliminated.

With Eqs. (11), (15) and (19), we can obtain the evolution equation of the system under feedback control and driving Hamiltonian as

$$\begin{aligned}\mathrm{d}\rho &= \Omega_0\rho\Omega_0^{\dagger}-\rho+\sum_{j=1}^{2}U_j\Omega_j\rho\Omega_j^{\dagger}U_j^{\dagger}\\ &= -\gamma_1\mathrm{d}tZ\otimes I(I\otimes I-Y\otimes Y)\rho\\ &\quad-\gamma_2\mathrm{d}tI\otimes Z(I\otimes I-Y\otimes Y)\rho\\ &\quad-\gamma_1\mathrm{d}t\rho(I\otimes I-Y\otimes Y)Z\otimes I\\ &\quad-\gamma_2\mathrm{d}t\rho(I\otimes I-Y\otimes Y)I\otimes Z\\ &\quad-\mathrm{i}[H_0,\rho]\mathrm{d}t+O(\mathrm{d}t^2).\end{aligned}\tag{20}$$

It is not hard to see that the code space can be protected by our scheme. However, for the simultaneous estimation of the three components of the magnetic field, the scheme with only feedback control and driving Hamiltonian is not sufficient. A fundamental problem is that the optimal protocols corresponding to each parameter are incompatible, which makes it impossible to achieve the highest precision for the simultaneous estimation of all three parameters. In the noiseless case, for each parameter $g\in\{x_1,x_2,x_3\}$, the Heisenberg uncertainty relation gives a fundamental limit on the estimation precision as

$$\delta g^2\geq\frac{1}{4\langle\Delta h_g^2\rangle},\tag{21}$$

where $\langle\Delta h_g^2\rangle=\langle\psi_g\mid h_g^2\mid\psi_g\rangle-\langle\psi_g\mid h_g\mid\psi_g\rangle^2$ is the variance of h_g, $h_g=\mathrm{i}(\partial_g U_g)U_g^{\dagger}$ is the generator of parameter translation $U_g=\mathrm{e}^{-\mathrm{i}tH_g}$ with respect to g, H_g is the Hamiltonian that encodes the parameter g, and t is the unit sensing time. Assuming that the total sensing time is $T=Nt$. Then, $h_g^{(N)}=\mathrm{i}(\partial_g U_g^N)(U_g^N)^{\dagger}=\sum_{k=0}^{N-1}U_g^k h_g(U_g^k)^{\dagger}$ holds and the variance of $h_g^{(N)}$ has the upper bound as

$$\langle\Delta[h_g^{(N)}]^2\rangle\leq N^2\langle\Delta h_g^2\rangle.\tag{22}$$

It can be seen that $h_g^{(N)}=Nh_g$ holds if U_g commutes with h_g. Thus, the upper bound of the variance of $h_g^{(N)}$ in Eq. (22) is saturated. In order to achieve the highest estimation precision for all parameters, U_g needs to commute with the generators h_{x_1}, h_{x_2}, h_{x_3} of all parameters simultaneously. However, this condition is almost impossible to be satisfied without any additional controls. Conversely, if there exists additional controls to make the total evolution of the system equal to $U_{\mathrm{tot}}=I$, then since $U_{\mathrm{tot}}=I$ commutes with all generators, we can solve this fundamental problem. It is necessary to emphasize that such controls actually exist. In particular, we can choose $U_{\mathrm{c}}=U_g^{\dagger}$. In this case, $U_{\mathrm{tot}}=U_{\mathrm{c}}U_g=I$.

Accordingly, the optimal control in our scheme can be chosen as $H_{\mathrm{c}}=-\boldsymbol{B}\cdot\boldsymbol{\sigma}^{(1)}$. The introduction of H_{c} can not only completely protect the code space, but also solve the incompatibility problem between multiple parameters. However, since $\boldsymbol{B}$ contains the parameters to be estimated, their true values are unknown before estimation. In this paper, we use their estimated values $\hat{\boldsymbol{B}}$ alternatively. To this end, we introduce an additional control of the form

$$H_{\mathrm{add}}=-\hat{\boldsymbol{B}}\cdot\boldsymbol{\sigma}^{(1)}.\tag{23}$$

It is easy to see that H_{add} needs to be updated adaptively according to the estimated values of the parameters. We adopt a sequential scheme to obtain the additional control, that is, an additional control H_{add} is added for every time interval $\mathrm{d}t$. The master equation (20) with the additional control can be rewritten as

$$\mathrm{d}\rho=-\mathrm{i}[\mathrm{d}H,\rho]\mathrm{d}t,\tag{24}$$

where $\mathrm{d}H\approx((B-\hat{B})(\sin\theta\cos\phi,\sin\theta\sin\phi,\cos\theta))\cdot\boldsymbol{\sigma}^{(1)}=(\mathrm{d}B(\sin\theta\cos\phi,\sin\theta\sin\phi,\cos\theta))\cdot\boldsymbol{\sigma}^{(1)}$. To simplify analysis, we assume that the additional control affects the three components of the magnetic field mainly by changing the magnitude of B.

We have known that the optimal measurement is the projective measurement on the Bell basis $(|\varphi_1\rangle,|\varphi_2\rangle,|\varphi_3\rangle,|\varphi_4\rangle)$, where $|\varphi_1\rangle=(|00\rangle-|11\rangle)/\sqrt{2}$, $|\varphi_2\rangle=(|00\rangle+|11\rangle)/\sqrt{2}$, $|\varphi_3\rangle=(|01\rangle-|10\rangle)/\sqrt{2}$, $|\varphi_4\rangle=(|01\rangle+|10\rangle)/\sqrt{2}$.[37] Therefore, the measurement operators can be selected as $M_1=|\varphi_1\rangle\langle\varphi_1|$, $M_2=|\varphi_2\rangle\langle\varphi_2|$, $M_3=|\varphi_3\rangle\langle\varphi_3|$, and $M_4=|\varphi_4\rangle\langle\varphi_4|$.

The initial probe state $|\psi_0\rangle$ undergoes the evolution described by Eq. (24) for some period T, and then the projective

measurements on the Bell basis are applied to the system. The probability of the measurement results can be obtained as

$$\begin{cases} p_{\mathrm{m1}} = \cos^2(T\mathrm{d}B), \\ p_{\mathrm{m2}} = \sin^2(T\mathrm{d}B)\cos^2\theta, \\ p_{\mathrm{m3}} = \sin^2(T\mathrm{d}B)\sin^2\theta\cos^2\phi, \\ p_{\mathrm{m4}} = \sin^2(T\mathrm{d}B)\sin^2\theta\sin^2\phi. \end{cases} \tag{25}$$

From Eq. (3), we can obtain the CFIM corresponding to the parameters (B,θ,ϕ) as follows (see detailed derivations in Appendix B):

$$F_{\mathrm{cl}} = 4\begin{pmatrix} T^2 & 0 & 0 \\ 0 & \sin^2(T\mathrm{d}B) & 0 \\ 0 & 0 & \sin^2(T\mathrm{d}B)\sin^2\theta \end{pmatrix}. \tag{26}$$

According to Eq. (2), the estimation precision corresponding to (B,θ,ϕ) has the following lower bounds:

$$\begin{cases} \delta\hat{B}^2 \geq \frac{1}{4T^2}, \\ \delta\hat{\theta}^2 \geq \frac{1}{4\sin^2(T\mathrm{d}B)}, \\ \delta\hat{\phi}^2 \geq \frac{1}{4\sin^2(T\mathrm{d}B)\sin^2\theta}. \end{cases} \tag{27}$$

In order to intuitively show the estimation precision corresponding to each component of the magnetic field, we rewrite the Hamiltonian encoding the parameters to be estimated as $H_0 = x_1X_1 + x_2Y_1 + x_3Z_1$, where $x_1 = B\sin\theta\cos\phi$, $x_2 = B\sin\theta\sin\phi$, and $x_3 = B\cos\theta$. The precision of each component of the magnetic field is $\delta\hat{x}_1 = \sin\theta\cos\phi\delta\hat{B} + B\cos\theta\cos\phi\delta\hat{\theta} - B\sin\theta\sin\phi\delta\hat{\phi}$, $\delta\hat{x}_2 = \sin\theta\sin\phi\delta\hat{B} + B\cos\theta\sin\phi\delta\hat{\theta} - B\sin\theta\cos\phi\delta\hat{\phi}$, $\delta\hat{x}_3 = \cos\theta\delta\hat{B} - B\sin\theta\delta\hat{\theta}$, respectively. As described in Subsection 2.1, we take the weight matrix as $W = I$, and the corresponding WMSE C is shown in Eq. (6). Plugging Eq. (27) into Eq. (6), we can obtain the minimum value of the WMSE (i.e., the estimation precision limit) corresponding to the simultaneous estimation of the three components of the magnetic field as

$$\begin{aligned} \delta\hat{x}_1^2 + \delta\hat{x}_2^2 + \delta\hat{x}_3^2 &= \delta\hat{B}^2 + \mathrm{d}B^2\delta\hat{\theta} + \mathrm{d}B^2\sin^2\theta\delta\hat{\phi}^2 \\ &= \frac{1}{4}\left(\frac{1}{T^2} + \frac{2\mathrm{d}B^2}{\sin^2(T\mathrm{d}B)}\right). \end{aligned} \tag{28}$$

When $\hat{\boldsymbol{B}} \to \boldsymbol{B}$, the additional control results in $\mathrm{d}B \to 0$. Thus, we have $\frac{\mathrm{d}B^2}{\sin^2(T\mathrm{d}B)} \to \frac{1}{T^2}$ and $\delta\hat{x}_1^2 + \delta\hat{x}_2^2 + \delta\hat{x}_3^2 \to \frac{3}{4T^2}$. It has been known that the highest estimation precision is $\frac{1}{4T^2}$ for a single parameter in the magnetic field.[15] If the three parameters reach the highest estimation accuracy, then the minimum value of WMSE is equal to $\frac{3}{4T^2}$. This implies that our scheme can achieve the highest estimation precision asymptotically for each parameter.

Figure 1 shows the performance of our scheme, especially the effect of the additional control. As can be seen from Fig. 1, the additional control can significantly enhance the multi-parameter estimation precision. Moreover, even if the parameters in the additional control are not very close to the true values at the beginning, it does not affect the HL of the multi-parameter estimation.

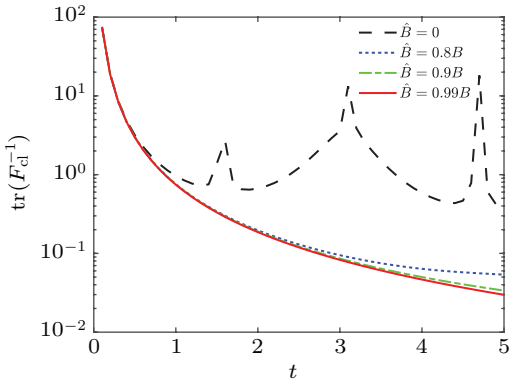


Fig. 1. Classical Cramér–Rao bound (CCRB) $\mathrm{tr}(F_{\mathrm{cl}}^{-1})$ versus the evolution time t is plotted. The black dashed line represents the case with feedback control and driving Hamiltonian. The blue dotted line, green dashed line, and red solid line indicate the cases with feedback control, driving Hamiltonian, and additional control, where the corresponding parameter value in the additional control is $\hat{B} = 0.8B$, $\hat{B} = 0.9B$, and $\hat{B} = 0.99B$ respectively, the true value of $\boldsymbol{x} = (B,\theta,\phi)$ to be estimated is set as $(1,1,1)$, and the values of other parameters are $\gamma_1 = \gamma_2 = 0.1$.

4. Conclusion

We explored the application of feedback control and quantum error correction to quantum multi-parameter estimation. One of the main challenges is decoherence caused by the environment such as spontaneous emission, which leads to the error in qubits. Our research shows that as long as the error can be detected, the encoded state can be maintained in the code space by the feedback control and QEC scheme in this paper and thereby the estimation precision of parameters can be improved. Compared with existing QEC schemes, our scheme does not require the ancilla system to be noiseless, and the dimensionality of the code space is greatly reduced. In a two-qubit system with spontaneous emission, our scheme achieves the highest simultaneous estimation precision for the three components of the magnetic field with only a two-dimensional code space. It should be pointed out that the types of errors that can be corrected decrease although the dimension of the code space is reduced. In future research, we will apply the combined control scheme to more complex quantum parameter estimation scenarios, e.g., the case of time-dependent parameter estimation.

Appendix A: The optimal probe state

Here, we detail the selection of the optimal probe state for simultaneous estimation of the three components of the magnetic field. The corresponding Hamiltonian has the form of

$$H_0 = x_1X_1 + x_2Y_1 + x_3Z_1, \tag{A1}$$

where x_1, x_2, and x_3 are the parameters to be estimated. Since the highest parameter estimation precision can only be achieved in the absence of noises, the corresponding optimal initial probe state $|\psi_{\rm opt}(0)\rangle$ is a pure state. The precision limit of multi-parameter estimation is bounded by the quantum Fisher information matrix (QFIM). For the pure state $|\psi(0)\rangle$, the elements of QFIM are

$$\begin{aligned}(F_Q)_{jk} = 4\mathrm{Re}(&\langle\partial_j\psi(T)\,|\,\partial_k\psi(T)\rangle \\ &-\langle\partial_j\psi(T)\,|\,\psi(T)\rangle\langle\psi(T)\,|\,\partial_k\psi(T)\rangle),\end{aligned} \tag{A2}$$

where $|\psi(T)\rangle = \mathrm{e}^{-\mathrm{i}H_0T}|\psi(0)\rangle$ is the system state at time T. By using Eq. (A2), the entries of QFIM can be calculated as

$$\begin{cases}(F_Q)_{x_1x_1} = 4T^2(1-\langle\psi(0)\,|\,X_1\,|\,\psi(0)\rangle), \\ (F_Q)_{x_2x_2} = 4T^2(1-\langle\psi(0)\,|\,Y_1\,|\,\psi(0)\rangle), \\ (F_Q)_{x_3x_3} = 4T^2(1-\langle\psi(0)\,|\,Z_1\,|\,\psi(0)\rangle), \\ (F_Q)_{x_1x_2} = 4T^2(\langle\psi(0)\,|\,X_1Y_1\,|\,\psi(0)\rangle \\ \qquad -\langle\psi(0)\,|\,X_1\,|\,\psi(0)\rangle\langle\psi(0)\,|\,Y_1\,|\,\psi(0)\rangle), \\ (F_Q)_{x_1x_3} = 4T^2(\langle\psi(0)\,|\,X_1Z_1\,|\,\psi(0)\rangle \\ \qquad -\langle\psi(0)\,|\,X_1\,|\,\psi(0)\rangle\langle\psi(0)\,|\,Z_1\,|\,\psi(0)\rangle), \\ (F_Q)_{x_2x_3} = 4T^2(\langle\psi(0)\,|\,Y_1Z_1\,|\,\psi(0)\rangle \\ \qquad -\langle\psi(0)\,|\,Y_1\,|\,\psi(0)\rangle\langle\psi(0)\,|\,Z_1\,|\,\psi(0)\rangle).\end{cases} \tag{A3}$$

In order to achieve the highest estimation precision for each parameter, the corresponding QFIM should be a diagonal matrix of the following form:

$$F_{Q_{\max}} = 4T^2 I. \tag{A4}$$

With Eqs. (A4) and (A3), it is not difficult to see that the optimal initial probe state needs to satisfy

$$\begin{cases}\langle\psi_{\rm opt}(0)|X_1|\psi_{\rm opt}(0)\rangle = 0, \\ \langle\psi_{\rm opt}(0)|Y_1|\psi_{\rm opt}(0)\rangle = 0, \\ \langle\psi_{\rm opt}(0)|Z_1|\psi_{\rm opt}(0)\rangle = 0.\end{cases} \tag{A5}$$

Denote the optimal initial probe state as $|\psi_{\rm opt}(0)\rangle = a|00\rangle + b|01\rangle + c|10\rangle + d|11\rangle$ (a, b, and c are complex numbers). Then, Eq. (A5) is equivalent to

$$\begin{cases}a^*c + b^*d + c^*a + d^*b = 0, \\ a^*c + b^*d - c^*a - d^*b = 0, \\ |a|^2 + |b|^2 - |c|^2 - |d|^2 = 0.\end{cases} \tag{A6}$$

Considering that the initial probe state satisfies $|a|^2 + |b|^2 + |c|^2 + |d|^2 = 1$, we have

$$\begin{cases}|a|^2 + |b|^2 = \dfrac{1}{2}, \\ |c|^2 + |d|^2 = \dfrac{1}{2}, \\ a^*c + b^*d = 0, \\ c^*a + d^*b = 0.\end{cases} \tag{A7}$$

It is easy to see that any maximum entangled state satisfies this condition. Hence, the optimal initial detection state can be selected as

$$|\psi_{\rm opt}(0)\rangle = \frac{1}{\sqrt{2}}(|00\rangle \pm |11\rangle) \tag{A8}$$

or

$$|\psi_{\rm opt}(0)\rangle = \frac{1}{\sqrt{2}}(|01\rangle \pm |10\rangle). \tag{A9}$$

Appendix B: Calculation of CFIM

As described in the main text, our control scheme maintains the encoded state in the code space. The evolution equation is shown in Eq. (24). The evolution can also be described by a unitary operator as $U(\boldsymbol{x},T) = \mathrm{e}^{-\mathrm{i}T\mathrm{d}H} \otimes I$, where $\mathrm{d}H \approx ((B-\hat{B})(\sin\theta\cos\phi, \sin\theta\sin\phi, \cos\theta)) \cdot \boldsymbol{\sigma}^{(1)} = \mathrm{d}B\sin\theta\cos\phi X_1 + \mathrm{d}B\sin\theta\sin\phi Y_1 + \mathrm{d}B\cos\theta Z_1$.

We choose the optimal initial probe state as $|\psi(0)\rangle = \frac{(|00\rangle - |11\rangle)}{\sqrt{2}} = \frac{1}{\sqrt{2}}\left(\begin{bmatrix}0\\1\end{bmatrix} \otimes \begin{bmatrix}0\\1\end{bmatrix} - \begin{bmatrix}1\\0\end{bmatrix} \otimes \begin{bmatrix}1\\0\end{bmatrix}\right)$. For some time T, the system undergoes the evolution $U(\boldsymbol{x},T)$. Then, the system state becomes

$$\begin{aligned}&|\psi(T)\rangle = U(\boldsymbol{x},T)|\psi(0)\rangle \\ &= \frac{1}{\sqrt{2}}\begin{bmatrix}-\mathrm{i}\sin(T\mathrm{d}B)\sin\theta\mathrm{e}^{-\mathrm{i}\phi} \\ \cos(T\mathrm{d}B) + \mathrm{i}\sin(T\mathrm{d}B)\cos\theta\end{bmatrix} \otimes \begin{bmatrix}0\\1\end{bmatrix} \\ &\quad - \frac{1}{\sqrt{2}}\begin{bmatrix}\cos(T\mathrm{d}B) - \mathrm{i}\sin(T\mathrm{d}B)\cos\theta \\ -\mathrm{i}\sin(T\mathrm{d}B)\sin\theta\mathrm{e}^{\mathrm{i}\phi}\end{bmatrix} \otimes \begin{bmatrix}1\\0\end{bmatrix}.\end{aligned} \tag{B1}$$

In the Bell basis, Eq. (B1) can be rewritten as

$$\begin{aligned}|\psi(T)\rangle = &\cos(T\mathrm{d}B)\left(\frac{|00\rangle - |11\rangle}{\sqrt{2}}\right) \\ &+ \mathrm{i}\sin(T\mathrm{d}B)\cos\theta\left(\frac{|00\rangle + |11\rangle}{\sqrt{2}}\right) \\ &+ \mathrm{i}\sin(T\mathrm{d}B)\sin\theta\cos\phi\left(\frac{|01\rangle - |10\rangle}{\sqrt{2}}\right) \\ &- \sin(T\mathrm{d}B)\sin\theta\sin\phi\left(\frac{|01\rangle + |10\rangle}{\sqrt{2}}\right).\end{aligned} \tag{B2}$$

After simple calculation, we can obtain the probability of the measurement result with the Bell basis as Eq. (25). By substituting it into Eq. (3), the CFIM can be obtained as shown in Eq. (26).

Acknowledgement

Project supported by the National Natural Science Foundation of China (Grant No. 61873251).

References

[1] Giovannetti V, Lloyd S and Maccone L 2004 *Science* **306** 1330
[2] Sugiyama T 2015 *Phys. Rev. A* **91** 042126
[3] Giovannetti V, Lloyd S and Maccone L 2011 *Nat. Photonics* **5** 222
[4] Wasilewski W, Jensen K, Krauter H, Renema J J, Balabas M V and Polzik E S 2010 *Phys. Rev. Lett.* **104** 133601

[5] Jiao Y C, Zhao J M and Jia S T 2018 *Acta Phys. Sin.* **67** 073201 (in Chinese)
[6] Danilishin S L and Khalili F Y 2012 *Living Rev. Relativ.* **15** 5
[7] Cole J H, Greentree A D, Oi D K L, Schirmer S G, Wellard C J and Hollenberg L C L 2006 *Phys. Rev. A* **73** 062333
[8] Shabani A, Mohseni M, Lloyd S, Kosut R L and Rabitz H 2011 *Phys. Rev. A* **84**012107
[9] Xie H T, Chen B, Long J B, Xue C, Chen L K and Chen S 2020 *Chin. Phys. B* **29** 093701
[10] Taylor M A and Bowen W P 2016 *Phys. Rep.* **615** 1
[11] Xiang G Y, Higgins B L, Berry D W, Wiseman H M and Pryde G J 2010 *Nat. Photonics* **5** 43
[12] Martínez-Vargas E, Pineda C Leyvraz F and Barberis-Blostein P 2017 *Phys. Rev. A* **95** 012136
[13] Pezzè L, Smerzi A, Oberthaler M K, Schmied R and Treutlein P 2018 *Rev. Mod. Phys.* **90** 035005
[14] Pezzè L, CiampiniM A, Spagnolo N, Humphreys P C, Datta A, Walmsley I A, Barbieri M, Sciarrino F and Smerzi A 2017 *Phys. Rev. Lett.* **119** 130504
[15] Yuan H and Fung C H F 2015 *Phys. Rev. Lett.* **115** 110401
[16] Sekatski P, Skotiniotis M, Kołodyński J and Dür W 2017 *Quantum* **1** 27
[17] Naghiloo M, Jordan A N and Murch K W 2017 *Phys. Rev. Lett.* **119** 180801
[18] Pang S and Brun T A 2014 *Phys. Rev. A* **90** 022117
[19] Pang S and Jordan A N 2017 *Nat. Commun.* **8** 14695
[20] Liu J and Yuan H 2017 *Phys. Rev. A* **96** 012117
[21] Xu H, Li J, Liu L, Wang Y, Yuan H and Wang X 2019 *npj Quantum Inf.* **5** 82
[22] Zhi H and Chun-Mei Y 2014 *Chin. Phys. B* **23**110601
[23] Nöbauer T, Angerer A, Bartels B, Trupke M, Rotter S, Schmiedmayer J, Mintert F and Majer J 2015 *Phys. Rev. Lett.* **115** 190801
[24] Häberle T, Schmid-Lorch D, Karrai K, Reinhard F and Wrachtrup J 2013 *Phys. Rev. Lett.* **111** 170801
[25] Yoshimura K G and Yamamoto N 2019*J. Phys. B: Atom. Mol. Opt. Phys.* **52** 055501
[26] Yu M and Fang M F 2017 *Int. J. Theor. Phys.* **56** 1937
[27] Zheng Q, Ge L, Yao Y and Zhi Q J 2015 *Phys. Rev. A* **91** 033805
[28] Hu Y H, Cao L M, Yang H F, Tan Y G and Wu Q 2020 *Laser Phys. Lett.* **17**035208
[29] Yang H Y, Zheng Q and Zhi Q J 2017 *Chin. Phys. B* **26** 010601
[30] Liu L and Yuan H 2020 *Phys. Rev. A* **102** 012208
[31] Humphreys P C, Barbieri M, Datta A and Walmsley I A 2013 *Phys. Rev. Lett.* **111** 070403
[32] Vaneph C, Tufarelli T and Genoni M G 2013 *Quantum Meas. Quantum Metro.* **1** 12
[33] Vidrighin M D, Donati G, Genoni M G, Jin X M, Kolthammer W S, Kim M, Datta A, Barbieri M and Walmsley I A 2013 *Nat. Commun.* **5** 3532
[34] Crowley P J D, Datta A, Barbieri M and Walmsley I A 2014 *Phys. Rev. A* **89** 023845
[35] Zhang Y R and Fan H 2014 *Phys. Rev. A* **90** 043818
[36] Baumgratz T and Datta A 2016 *Phys. Rev. Lett.* **116** 030801
[37] Yuan H 2016 *Phys. Rev. Lett.* **117** 160801
[38] Hou Z, Tang J F, Chen H, Yuan H, Xiang G Y, Li C F and Guo G C 2021 *Sci. Adv.* **7** eabd2986
[39] Górecki W, Zhou S, Jiang L and Demkowicz-Dobrzański R 2020 *Quantum* **4** 288
[40] Zhou S, Zhang M, Preskill J and Jiang L 2018 *Nat. Commun.* **9**78
[41] Zhou S and Jiang L 2020 *Phys. Rev. Res.* **2** 013235
[42] Layden D, Zhou S, Cappellaro P and Jiang L 2019 *Phys. Rev. Lett.* **122** 040502
[43] Dür, W, Skotiniotis, M, Fröwis F and Kraus B 2014 *Phys. Rev. Lett.* **112**080801
[44] Matsuzaki Y and Benjamin S 2017 *Phys. Rev. A* **95** 032303
[45] Ragy S, Jarzyna M and Demkowicz-Dobrzański R 2016 *Phys. Rev. A* **94** 052108
[46] Demkowicz-Dobrzański R, Górecki W and Guţă M 2020 *J. Phys. A* **53** 363001
[47] Wiseman H M 1994 *Phys. Rev. A* **49** 2133
[48] Gottesman D 1998 *Phys. Rev. A* **57** 127
[49] Knill E and Laflamme R 1997 *Phys. Rev. A* **55** 900